The current issue and full text archive of this journal is available at
www.emeraldinsight.com/0961-5539.htm

Analysis of macroscopic momentum equation in a columnar mushy zone

Piotr Furmański and Jerzy Banaszek
Institute of Heat Engineering, Warsaw University of Technology, Warszawa, Poland

Received 5 December 2006
Revised 25 May 2007
Accepted 25 May 2007

Abstract

Purpose – This paper aims to tackle the problem of some ambiguity of the momentum equation formulation in the commonly used macroscopic models of two-phase solid/liquid region, developing during alloy solidification. These different appearances of the momentum equation are compared and the issue is addressed of how the choice of the particular form affects velocity and temperature fields.

Design/methodology/approach – Attention is focused on the ensemble averaging method, which, owing to its stochastic nature, is a new promising tool for setting up the macroscopic transport equations in highly inhomogeneous multiphase micro- and macro-structures, with morphology continuously changing in time when the solidification proceeds. The basic assumptions of the two other continuum models, i.e. based on the classical mixture theory and on the volume-averaging technique, are also unveiled. These three different forms of the momentum equation are then compared analytically and their impact on calculated velocity and temperature distribution in the mushy zone is studied for the selected test problem of binary alloy solidification driven by diffusion and thermal natural convection in a square mould.

Findings – It is found that a chosen appearance of the momentum equation mildly affects temporal velocity/temperature, and shapes of the phase interface at longer times of the solidification.

Research limitations/implications – This mainly results from small variations of the liquid fraction across the mushy zone and from a low solidification rate, and it may change drastically when anisotropic properties of the mushy zone, solutal convection, different phase densities and cooling conditions are considered. Therefore, further comprehensive study is needed.

Originality/value – The paper addresses how the different focus of the momentum equation for liquid flow is compared.

Keywords Solidification, Numerical analysis, Simulation, Flow

Paper type Research paper

Nomenclature

f_l	= liquid mass fraction	μ_l	= liquid viscosity
g	= specific gravity	μ_{l^*}	= effective liquid viscosity
K	= permeability of the mushy zone	ρ_s	= solid density
p	= pressure	ρ_l	= liquid density
T	= temperature	$\boldsymbol{\sigma}$	= stress tensor
T_{ref}	= reference temperature	θ_l	= structure function
w	= liquid velocity	$\mathbf{1}$	= unit tensor
w_i	= liquid-solid interphase velocity	$\{\ldots\}$	= superficial average
β_{Tl}	= liquid thermal expansion coefficient	$\{\ldots\}_m$	= mass average
ε_l	= liquid volume fraction	$\{\ldots\}_l$	= liquid intrinsic average

This paper was partially financed by the State Committee of Scientific Research under Grant No. 1472/T10/2005/29.

International Journal of Numerical Methods for Heat & Fluid Flow
Vol. 18 No. 3/4, 2008
pp. 533-544

0961-5539
DOI 10.1108/09615530810853718

1. Introduction

Solidification of binary alloys occurs over a temperature range and is associated with formation of a mushy zone, i.e. two-phase solid/liquid region. In general, two distinct dendritic structures can be distinguished in the mushy zone, i.e. the columnar and the equiaxed ones. The former grows from a mould wall and has a strongly directional nature. The equiaxed structure is formed in the undercooled liquid and it has more isotropic character. Transfer processes occurring in the mushy zone contribute to formation of these two different microstructures and the transition from one to another in a cast. Among them, heat conduction and solute diffusion in both phases, generation of heat and segregation of species at the interface as well as heat convection in the liquid are fundamental in the microstructure formation.

Thermo-solutal convection of the inter-dendritic fluid in the mushy zone and fully liquid region is known to significantly affect the rate of solidification, the shape of phase front and formation of chimney effects in the mushy zone. It is also responsible for micro- and macro-segregation of the alloying components thus contributing to their redistribution in the material. This in turn influences microstructure and quality of the final product.

Owing to complex microstructure, transfer processes in the mushy zone are analysed on the macroscopic scale where local variation of temperature, species concentration or fluid velocity are smoothed out (Furmanski, 2004). Movement of liquid in the mushy zone is predicted with the help of continuity and momentum equations. During the last several years, different forms of the macroscopic momentum equation were proposed (Furmanski, 2004; Bennon and Incropera, 1987; Ganesan and Poirier, 1990) for the columnar mushy zone. They were derived on the basis of three different continuum models for the mushy zone, i.e. the classical mixture theory (Bennon and Incropera, 1987; Prescott *et al.*, 1991; Sinha and Sundarajan, 1992), the volume averaging technique (Ganesan and Poirier, 1990; Beckermann and Viskanta, 1993; Bousquet-Melou *et al.*, 2002) and the ensemble averaging technique (Furmanski, 2004; Banaszek *et al.*, 2005). The literature suggests some ambiguity in the formulation and application of the momentum equation. As noted in Ganesan and Poirier (1990) and Prescott *et al.* (1991), although several different momentum equations for treating inter-dendritic flow can be found in literature, little fundamental justification has been provided for the models. Reassessment of the momentum equation allowed for comparison of the mixture and the volume averaging models (Prescott *et al.*, 1991). The general conclusion is that both models are equally suited to be implemented and they give similar results (Prescott *et al.*, 1991; Bousquet-Melou *et al.*, 2002). The volume averaging model is found to be more preferable due to its ability to show how microscopic phenomena influence macroscopic behaviour and to the development of micro-macroscopic models. However, the final evaluation of some phase interaction terms in the volume averaging model, in terms of the microscopic variables used in its description, is still impossible since these variables cannot be resolved in a macroscopic model (Prescott *et al.*, 1991).

The objective of the present paper is the extension of discussion on the assumptions made and the obtained appearances of the momentum equation in the mushy zone, to the form resulting from the ensemble averaging technique (Furmanski, 2004; Banaszek *et al.*, 2005). Moreover, an example of columnar binary alloy solidification is calculated to study the impact of different forms of this equation on temporary velocity and temperature fields.

The paper focuses only on the momentum equation which is the one from the set of fundamental conservation equations of mass, momentum, solute concentration and energy used in numerical simulations. Micro-segregation is included in such a model by closing relationship between volumetric solid fraction and temperature (and in the more enhanced models the influence of a dendrite tip velocity is taken into account). This issue, however, goes beyond the subject of the paper.

2. Continuity and momentum equations for the mushy zone

In most derivations of the continuity and momentum equations, a stationary solid phase and Newtonian fluid are assumed. Three, differently defined, macroscopic velocities are used. The intrinsic liquid velocity $\{w\}_{\mathbf{l}}$ describes the macroscopic velocity averaged solely over the liquid phase. The superficial (also Darcy or filtration) velocity $\{w\}$ denotes the macroscopic velocity averaged over both phases and is related to the previous one by the formula (Beckermann and Viskanta, 1993; Banaszek *et al.*, 2005):

$$\{w\} = \varepsilon_{\mathrm{l}}\{w\}_{\mathrm{l}} \tag{1}$$

where ε_{l} stands for the porosity of the two-phase region (liquid volume fraction in the mush). Finally, the mass average velocity $\{w\}_{\mathrm{m}}$ is defined as:

$$\{w\}_{\mathrm{m}} = f_{\mathrm{l}}\{w\}_{\mathrm{l}} \tag{2}$$

The symbol f_{l} is the mass fraction of liquid related to the volume fraction by:

$$f_{\mathrm{l}} = \frac{\rho_{\mathrm{l}}}{\{\rho\}}\,\varepsilon_{\mathrm{l}} \tag{3}$$

where ρ_{l} denotes liquid, ρ_{s} solid and mixture $\{\rho\} = \varepsilon_{\mathrm{l}}\rho_{\mathrm{l}} + (1 - \varepsilon_{\mathrm{l}})\rho_{\mathrm{s}}$ densities, respectively.

All three ways of derivation of macroscopic equations lead to the common continuity equation, i.e.:

$$\partial_t\{\rho\} + \nabla\cdot(\rho_{\mathrm{l}}\varepsilon_{\mathrm{l}}\{w\}_{\mathbf{l}}) = \partial_t\{\rho\} + \nabla\cdot(\rho_{\mathrm{l}}\{w\}) = 0 \tag{4}$$

For the equal and constant densities of both phases, this equation reduces to:

$$\nabla\cdot(\varepsilon_{\mathrm{l}}\{w\}_{\mathbf{l}}) = \nabla\cdot\{w\} = 0 \tag{4a}$$

The major debate is associated with the appearance of the momentum equation in the mushy zone.

2.1 Mixture theory

The classical mixture theory assumes that the liquid and solid phases are totally mixed. The conservation equations for each phase are added and Newton's third law imposed to eliminate a net phase interaction force. Subsequently, expressions for the intrinsic phase stresses are assumed and the semi-empirical relationship for the drag force term postulated. This yields, in the case of thermal buoyancy induced convection, the following form of the momentum equation (Prescott *et al.*, 1991 – equation (16)):

$$[\partial_t\{\rho\}\{w\}_{\mathrm{m}} + \nabla\cdot(\{\rho\}\{w\}_{\mathrm{m}}\{w\}_{\mathrm{m}})] = -\varepsilon_{\mathrm{l}}\nabla\{p\}_{\mathrm{l}} + \mu_{\mathrm{l}}\nabla\cdot\left[\frac{\{\rho\}}{\rho_{\mathrm{l}}}(\nabla\{w\}_{\mathrm{m}} + \nabla^{\mathrm{T}}\{w\}_{\mathrm{m}})\right] + \varepsilon_{\mathrm{l}}\rho_{\mathrm{l}}g\beta_{\mathrm{Tl}}(\{T\} - T_{\mathrm{ref}}) - \mu_{\mathrm{l}}\varepsilon_{\mathrm{l}}\frac{\{\rho\}}{\rho_{\mathrm{l}}}K^{-1}\cdot\{w\}_{\mathrm{m}} \tag{5}$$

where $\{p\}_{\mathrm{l}}$ is the intrinsic pressure, μ_{l}, liquid viscosity; $\{T\}$, macroscopic (superficial) temperature; $\mathbf{T}_{\mathrm{ref}}$, reference temperature; K^{-1}, inverse of permeability and β_{Tl} denotes a coefficient of thermal expansion of the liquid.

In order to avoid changing existing codes by accounting for the scaling of the pressure gradient by ε_{l}, equation (5) can be transformed to the considered equivalent form (see Prescott *et al.*, 1991 – equation (17)):

$$[\partial_t\{\rho\}\{w\}_{\mathrm{m}} + \nabla\cdot(\{\rho\}\{w\}_{\mathrm{m}}\{w\}_{\mathrm{m}})] = -\nabla\{p\}_{\mathrm{l}} + \mu_{\mathrm{l}}\nabla\cdot\left[\frac{\{\rho\}}{\rho_{\mathrm{l}}}(\nabla\{w\}_{\mathrm{m}} + \nabla^{\mathrm{T}}\{w\}_{\mathrm{m}})\right] + \rho_{\mathrm{l}}g\beta_{\mathrm{Tl}}(\{T\} - T_{\mathrm{ref}}) - \mu_{\mathrm{l}}\frac{\{\rho\}}{\rho_{\mathrm{l}}}\mathbf{K}^{-1}\cdot\{w\}_{\mathrm{m}} \tag{5a}$$

2.2 Volume averaging method

In the volume averaging approach, the concept of a representative elementary volume (REV) is used. In the statistically homogeneous structures, on the macroscopic level, a REV dimension is assumed to be greater than the greatest characteristic length describing microstructure and at the same time much smaller than the domain considered. The microscopic conservation equations are integrated over the REV to get their respective macroscopic counterparts, valid in the whole domain. Phase interaction terms in these equations are represented by interfacial area integrals. These integrals are usually not calculated but they are rather represented by postulated semi-empirical relationships. This approach leads to the one of the two following representations of the macroscopic momentum equation. In accordance with Ganesan and Poirier (1990) (see equation (51) there), the equation takes:

$$\rho_{\mathrm{l}}\varepsilon_{\mathrm{l}}[\partial_t\{w\}_{\mathrm{l}} + \{w\}_{\mathrm{l}}\cdot\nabla\{w\}_{\mathrm{l}}] = -\varepsilon_{\mathrm{l}}\nabla\{p\}_{\mathrm{l}} + \mu_{\mathrm{l}}\nabla^2\{w\} + \varepsilon_{\mathrm{l}}\rho_{\mathrm{l}}g\beta_{\mathrm{Tl}}(\{T\} - T_{\mathrm{ref}}) - \mu_{\mathrm{l}}\varepsilon_{\mathrm{l}}K^{-1}\cdot\{w\} \tag{6}$$

whereas, in Beckermann and Viskanta (1993) (see equations (59) and (61) there), it is derived as:

$$\rho_{\mathrm{l}}\left[\partial_t\{w\} + \nabla\cdot\left(\varepsilon_{\mathrm{l}}^{-1}\{w\}\{w\}\right)\right] = -\varepsilon_{\mathrm{l}}\nabla\{p\}_{\mathrm{l}} + \mu_{\mathrm{l}}^{*}\nabla^2\{w\} + \varepsilon_{\mathrm{l}}\rho_{\mathrm{l}}g\beta_{\mathrm{Tl}}(\{T\} - T_{\mathrm{ref}}) - \mu_{\mathrm{l}}\varepsilon_{\mathrm{l}}K^{-1}\cdot\{w\} \tag{6a}$$

The effective liquid viscosity, μ_{l}^{*}, appearing in the above equation, is usually taken to be equal to the actual liquid viscosity (Beckermann and Viskanta, 1993).

However, the origin of this effective viscosity is not evident in the context of alloy solidification (Ganesan and Poirier, 1990).

Only in the case of regular, periodic structures can the respective relationships be mathematically justified. The evolving dendritic columnar mushy region is highly irregular and characterized by non-uniformity of the macroscopic properties. Therefore, the REV cannot be easily selected except for the case when the evolving macroscopic heterogeneities are very small; otherwise the deforming REV should be considered. This remains a real challenge in the volume averaging approach. Assuming small and moderate macroscopic heterogeneities and periodicity of the dendritic columnar microstructure in the mushy zone the following momentum equation was obtained (see Bousquet-Melou *et al.*, 2002 – equation (93))

$$\rho_l\left[\partial_t\{w\} + \nabla\cdot\left(\varepsilon_l^{-1}\{w\}\{w\}\right)\right] = -\varepsilon_l\nabla\{p\}_l + \mu_l\nabla^2\{w\} - \mu_l\nabla\varepsilon_l\cdot\nabla\left(\varepsilon_l^{-1}\{w\}\right) + \varepsilon_l\rho_l g\beta_{Tl}(\{T\} - T_{ref}) - \mu_l\varepsilon_l K^{-1}\cdot\{w\} \tag{7}$$

The second and third terms on the right hand side of equation (7) denote Brinkman corrections, which describe the influence of viscous forces on liquid flow in the mushy zone (Bousquet-Melou *et al.*, 2002). Higher order Forchheimer term (Bousquet-Melou *et al.*, 2002), dependent on the product of liquid velocities, is deliberately abandoned due to small liquid velocities in the mushy zone.

Equation (7) can be easily transformed into the appearance that resembles equation (5), i.e.:

$$\rho_l[\partial_t\{w\} + \nabla\cdot(\{w\}\{w\})] = -\varepsilon_l\nabla\{p\}_l + \mu_l\nabla^2\{w\} + \varepsilon_l\rho_l g\beta_{Tl}(\{T\} - T_{ref}) - \mu_l\varepsilon_l K^{-1}\cdot\{w\} + \nabla\varepsilon_l\cdot\left[-\mu_l\nabla\left(\varepsilon_l^{-1}\{w\}\right) + \rho_l\varepsilon_l^{-2}\{w\}\{w\}\right] + \rho_l(1-\varepsilon_l^{-1})\nabla\cdot(\{w\}\{w\}) \tag{7a}$$

Now, it may be noted that for slow variation of the liquid volume fraction, ε_l, in the mushy zone and small influence of the liquid inertia the fifth and sixth terms on the right hand side of equation (7a) might be dropped. If additionally, the same and constant densities of both phases are invoked, the equations (5) and (7a) become identical.

2.3 Ensemble averaging method

The ensemble averaging method is based on the concept of an ensemble of realizations (configurations) of the microstructure of the mushy zone. A separate configuration may be understood as a set of characteristic points, e.g. nucleation sites or places where the primary dendrite arms emerge, that are spread randomly all over a considered volume (Furmanski, 2004; Banaszek *et al.*, 2005). This approach does not need the notion of REV. Averaging of a field variable is carried over a set of such configurations to which a respective probability measure is applied. Any macroscopic, physical quantity appearing in the macroscopic equations (obtained within this method) is understood as a statistically mean value (the awaited value) defined at any point of the medium. The ensemble averaging can be applied to study heterogeneous media that are both homogeneous and non-homogeneous at the macroscopic scale.

The solid phase is assumed to be rigid and motionless. As force interaction between liquid and solid phase exists, the medium is not in mechanical equilibrium and it is

preferable to apply the ensemble averaging technique to each phase separately, i.e. to use the double continuum approach. Upon averaging the momentum equation over the liquid phase, the following is obtained (Banaszek *et al.*, 2005):

$$\begin{aligned}\partial_t(\varepsilon_l\rho_l\{w\}_l) + \nabla\cdot[\varepsilon_l(\rho_l\{ww\}_l - \{\boldsymbol{\sigma}\}_l)] - \varepsilon_l\rho_l g\beta_{Tl}(\{T\} - T_{ref}) \\ = \{\rho_l w(w - w_i)\cdot\nabla\theta_l\} - \{\boldsymbol{\sigma}_l\cdot\nabla\theta_l\}\end{aligned} \tag{8}$$

where $\boldsymbol{\sigma}_l$ and θ_l are the stress function in the liquid and the structure function, respectively. The latter function is equal to unity in the liquid phase and to zero in the solid one. The terms on the right hand side of the equation correspond to the advective and diffusive momentum transfer between phases, respectively.

In order to numerically solve the momentum conservation equation, equation (8), the relations between $\{ww\}_l$, $\{\boldsymbol{\sigma}\}_l$, $\{\rho_l w(w - w_i)\cdot\nabla\theta_l\}$, $\{\boldsymbol{\sigma}_l\cdot\nabla\theta_l\}$, the intrinsic velocity $\{w\}_l$, and the intrinsic pressure $\{p\}_l$ should be given. These constitutive relations could be derived if relationship between microscopic velocity w and pressure p in the liquid phase and the intrinsic velocity $\{w\}_l$ and pressure $\{p\}_l$ are known.

At first, the microscopic relation between stress tensor, velocity and pressure in the liquid phase is multiplied by the structure function θ_l and ensemble averaged leading to the expression:

$$\varepsilon_l\{\boldsymbol{\sigma}\}_l = -\varepsilon_l\{p\}_l\mathbf{1} + 2\mu_l\mathbf{e}(\varepsilon_l\{w\}_l) - \mu_l\{\nabla\theta_l w_l + w_l\nabla\theta_l\} \tag{9}$$

where $\mathbf{e}(w) = (\nabla w + \nabla^T w)/2$ is the deformation rate tensor.

When equation (9) is introduced into equation (8), the following relationship is obtained:

$$\begin{aligned}\partial_t(\varepsilon_l\rho_l\{w\}_l) + \nabla\cdot(\varepsilon_l\rho_l\{ww\}_l) = \nabla\cdot(\varepsilon_l\{p\}_l) + \mu_l\nabla^2(\varepsilon_l\{w\}_l) - \mu_l\nabla\cdot\{\nabla\theta_l w + w\nabla\theta_l\} \\ + \varepsilon_l\rho_l g\beta_{Tl}(\{T\} - T_{ref}) + \{(w - w_i)\rho_l w\cdot\nabla\theta_l\} \\ - \{[p\mathbf{1} - 2\mu_l\mathbf{e}(w)]\cdot\nabla\theta_l\}\end{aligned} \tag{10}$$

Next, introducing the pressure and velocity fluctuations as:

$$p' = p - \{p\}_l, \tag{11}$$

$$w' = w - \{w\}_l \tag{12}$$

multiplying the microscopic momentum equation, equation (8), by the volume fraction of the liquid phase, and then subtracting equation (10), the equation for local fluctuations of velocity and pressure is derived:

$$\begin{aligned}\varepsilon_l\partial_t(\rho_l w') + \varepsilon_l\nabla\cdot(\rho_l\{w\}_l w') + \varepsilon_l\nabla\cdot(\rho_l w'\{w\}_l) + \varepsilon_l\nabla\cdot(\rho_l w'w') - \nabla\cdot(\varepsilon_l\rho_l\{w'w'\}_l) \\ = -\varepsilon_l\nabla p' + \varepsilon_l\mu_l\nabla^2(w') + \{[-p'\mathbf{1} + 2\mu_l\mathbf{e}(w')]\cdot\nabla\theta\} + \mu_l\nabla\cdot\{\nabla\theta_l w' + w'\nabla\theta_l\} \\ - \{(w - w_i)\rho_l w'\cdot\nabla\theta_l\}\end{aligned} \tag{13}$$

Using the Green function theory, the following formal solution for the liquid velocity fluctuations is obtained from equation (13):

$$w' = \int_o^t \int_{V_l} G[\nabla p' + \rho_l w' \cdot \nabla \{w\}_l + \varepsilon_l^{-1}\{((\{w\}_l - w)\rho_l w'_{\mathbf{l}} + p'\mathbf{1} - 2\mu_l \mathbf{e}(w')) \cdot \nabla\theta_l\} - \varepsilon_l^{-1}\mu_l \nabla \cdot \{\nabla\theta_l w' + w'\nabla\theta_l\}]\mathrm{d}V'\mathrm{d}\tau - \int_0^t \int_{A_i} \mu_l[((1 - \rho_s/\rho_l)w' \cdot \mathbf{n} + \rho_s/\rho_l)w' \cdot \mathbf{n})\mathbf{n} + (w' \cdot \mathbf{t})\mathbf{t}]\nabla G \cdot \mathbf{n}\mathrm{d}A'\mathbf{d}\tau \quad (14)$$

where G is the respective Green function, while $\mathbf{n}$ and $\mathbf{t}$ are, respectively, normal and tangential unit vectors to the interface.

A general solution of the above equation leads to non-local form of the constitutive equations (Banaszek *et al.*, 2005). It is known that the microstructure and associated variations in local properties within the mushy zone can be described by many characteristic length scales. To these length scales belong transverse dimensions of dendrites, diameters of the equiaxed grains, radii of dendrite tips, spacing of the primary and secondary dendrite arms, characteristic lengths associated with variation of the correlation functions. If the greatest micro-length λ (e.g. the primary dendrite spacing) is smaller than the smallest characteristic macro-lengths, describing variations in the macroscopic (intrinsic) velocity and pressure fields, then significant simplifications in the constitutive relations can be attained. In fact, this assumption is equivalent to the postulation of a good separation between the spectrum of length scales describing the mushy zone microstructure and the spectrum of length scales describing variations in the macroscopic velocity and pressure fields. The following solution of the equation (14) can then be sought (Furmanski, 2004):

$$p_l = \{p\}_l + \ell\varphi_{p0} \cdot \{w\}_l + O(\ell^2) \quad (15)$$

$$w = \{w\}_l + \ell^2\psi_{w0} \cdot \{w\}_l + O(\ell^2) \quad (16)$$

where functions φ_{p0}, ψ_{w0} satisfy the following differential equation:

$$\psi_{w0}(\xi) = \int_{V_l} G_s(\xi, \eta)[-\varphi_{p0}(\eta) + \mu_l \mathbf{K}^{-1}]\mathrm{d}\eta \quad (17)$$

where the symbol G_s denotes a stationary form of the pertinent Green function. The above equation is written in local, non-dimensional coordinate system associated with the nearest to location x nucleation site $x'_{\mathbf{i}}$, i.e. $\xi = (x - x'_{\mathbf{i}})/\ell$ (Banaszek *et al.*, 2005).

Substituting equations (15) and (16) into (8), and neglecting the term dependent on product of velocity fluctuations, the macroscopic momentum equation, takes (Furmanski, 2004; Banaszek *et al.*, 2005):

$$\rho_l[\partial_t\{w\}_{\mathbf{l}} + \nabla \cdot (\{w\}_{\mathbf{l}}\{w\}_{\mathbf{l}})] = -\nabla\{p\}_l + \mu_l\nabla^2\{w\}_{\mathbf{l}} + \rho_l g\beta_{\mathbf{Tl}}(\{T\} - T_{\mathrm{ref}}) - \mu_l\varepsilon_l\mathbf{K}^{-1} \cdot \{w\}_{\mathbf{l}} \quad (18)$$

where the permeability tensor $\mathbf{K}$ is defined as:

$$\mathbf{K}^{-1} = \frac{\nu_{\mathrm{wef0}}}{\mu_l} = (\mu_l\varepsilon_l^{-1})^{-1}[\{[-\varphi_{p0}\mathbf{1} + 2\mu_l\mathbf{e}(\psi_{w0})] \cdot \nabla\theta_l\} + \mu_l\nabla \cdot \{\nabla\theta_l\psi_{w0} + \psi_{w0}\nabla\theta_l\}] \quad (19)$$

It may be noticed that equation (18) contains only the intrinsic liquid velocity. But, when the superficial liquid velocity, given by equation (1), is introduced in equation (18), this equation can be rewritten in the following equivalent form:

$$\begin{aligned}\rho[\partial_t\{w\} + \nabla\cdot(\{w\}\{w\})] = &-\varepsilon_l\nabla\{p\}_l + \mu_l\nabla^2\{w\} + \varepsilon_l\rho_l g\beta_{Tl}(\{T\} - T_{ref}) \\ &- \mu_l\varepsilon_l\boldsymbol{K}^{-1}\cdot\{w\} + \nabla\varepsilon_l\cdot\left[-\mu_l(\nabla\{\mathbf{w}\} + \nabla^T\{w\})\right. \\ &\left.+\mu_l\left(\frac{\nabla\varepsilon_l}{\varepsilon_l}\{w\} + \{w\}\frac{\nabla\varepsilon_l}{\varepsilon_l}\right) + 2\rho_l\varepsilon_l^{-2}\{w\}\{w\}\right] \\ &- \mu_l\nabla\cdot(\nabla\varepsilon_l\{w\} + \{w\}\nabla\varepsilon_l) \\ &+ \varepsilon_l^{-1}(\dot{m}_l - \rho_l\nabla\cdot\{w\})\{w\} \\ &+ \rho_l(\varepsilon_l - 1)\nabla\cdot(\{w\}\{w\})\end{aligned} \tag{20}$$

If $\nabla\varepsilon_l \ll 1$, small influence of the liquid inertia and solidification rate $\dot{m}_l$ as well as the same densities of both phases the above equation reduces to equation (5). This is, however, valid only if the liquid volume fraction, ε_l, varies slowly in the mushy zone, which is not necessary the case close to the solidus line.

3. Comparison of different forms of momentum equation

To compare temporal velocity and temperature fields provided by different forms of the macroscopic momentum equation, this equation has been coupled with the continuity equation, equation (4), and with the enthalpy version of energy equation (Voller and Swaminathan, 1992). Discrete counterpart of thus obtained mathematical representation has been established by using the control volume finite difference method (Patankar, 1980), where local mass, momentum and energy balances are set up on a control volume grid. The staggered grid technique (Patankar, 1980) has been used to avoid checkerboard pressure modes, along with the power-law upwinding to eliminate non-physical spatial oscillations of the numerical solution. The iterative segregated solution strategy has been adopted, where directional momentum equations and the energy equation are linearised and solved consecutively. To separately calculate pressure and velocity fields, Patankar's velocity and pressure correction method has been used (Voller and Swaminathan, 1992) along with the SIMPLEC computational algorithm (van Doormal and Raithby, 1984). The general enthalpy method (Voller and Swaminathan, 1992) has been applied to incorporate the latent heat effect on a fixed control-volume grid.

Two different representations of the macroscopic momentum equation have been incorporated into the above-described algorithm. The first is based on the mixture theory, equation (5), whereas the second one is built on the ensemble averaging approach, equation (18). They are further referred to as Models 1 and 2, respectively.

As a test example, solidification of a binary alloy was considered in a differentially heated rectangular mould (0.09 × 0.18 m). The staggered grid of 25 × 50 control volumes was used in discretization of the mould area. The bottom and top horizontal walls of the mould were assumed adiabatic, whereas the lateral walls were kept at constant, but different temperatures. The right hot wall had temperature $T_H = 700$°C

equal to the initial one, T_i. A sudden drop of the left wall temperature, from T_i to $T_C = 700$°C, initiated cooling and solidification of the binary solution in the mould.

For a chosen alloy, the liquidus and solidus temperatures are $T_l = 650$°C and $T_s = 550$°C, respectively, and the latent heat of fusion is $L = 400$ kJ/kg. Equal densities of both the solid and liquid phases were assumed, i.e.: $\rho_s = \rho_l = \rho = 2,500\,\mathrm{kg/m^3}$; viscosity $\mu_l = 2.5 \cdot 10^{-3}$ Pa s, thermal expansion coefficient of the liquid $\beta_{Tl} = 4.0 \cdot 10^{-5}\,\mathbf{K}^{-1}$. Constant and even specific heats and thermal conductivities of the both phases were assumed as $c_{pl} = c_{ps} = 1.0\,\mathrm{kJ/(kg\,K)}$ and $k_l = k_s = 100\,\mathrm{W/(m\,K)}$, respectively, while the latent heat of solidification as $L = 400$ kJ/kg. For calculation of the liquid volume fraction, the lever rule was adopted (Voller and Swaminathan, 1992) and isotropic permeability from Blake-Kozeny relation was used (Bennon and Incropera, 1987).

The results obtained are shown in Figures 1-3. The first figure compares temporal streamlines in the mushy zone and bulk liquid region for the two considered models of the momentum equation. Initially, differences between the streamlines of both models are indistinguishable. However, as solidification proceeds more differences appear. Flow intensity seems to be slightly less intensive in the second model. Temporal isotherms for both models are shown in Figure 2. Isotherms in the Model 2 move slower towards an upper part of the mould and faster in its bottom part.

Vertical velocities of the liquid phase in three horizontal cross-sections of the mould are shown in Figure 3 at three different times. Their temporal distributions confirm that although differences between two models of the momentum equation are initially small they grow in time. Generally, the Model 2 gives higher velocities in the mushy zone and in the bulk liquid region in comparison to the Model 1.

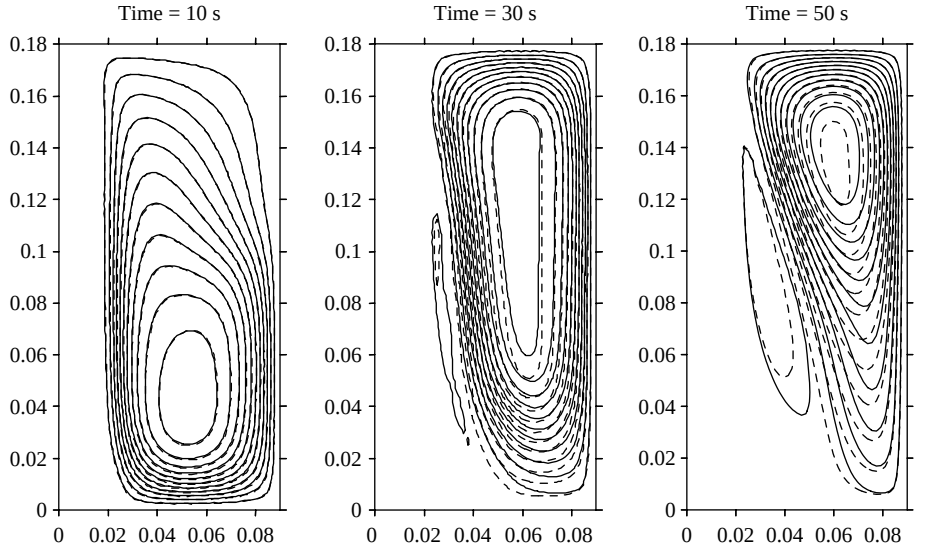

Notes: MODEL 1 – solid line; MODEL 2 – dashed line

Figure 1.
Streamlines at different times for different models of the momentum equation in the mushy zone

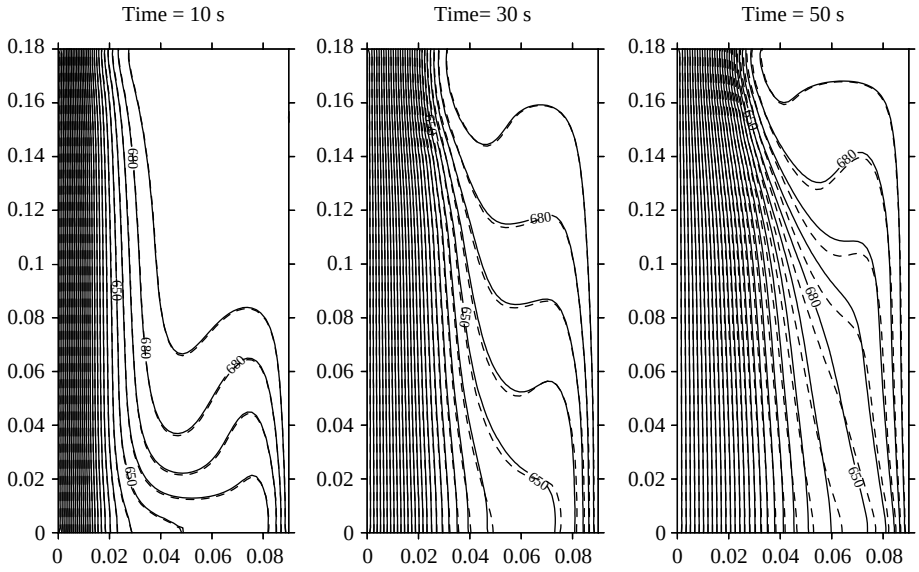

Figure 2.
Isotherms at different times for different models of the momentum equation in the mushy zone

Notes: MODEL 1 – solid line; MODEL 2 – dashed line

4. Conclusions

Different forms of the macroscopic momentum equation in the columnar mushy zone of a solidifying binary mixture were analysed and compared. It was found that although they had been derived in a different way and sometimes comprise different terms, they give essentially similar results for the liquid flow pattern, temperature distribution and phase change front shape. Small differences in the numerical results obtained seem to result mainly from small variations of the liquid fraction ε_l across the mushy zone and a slow solidification rate as discussed in the end of Section 2.3. These results match those presented in Furmański and Banaszek (2006) where the influence of permeability model on the solidification process is studied. They indicate that although permeability varies by up to two orders of magnitude, only small differences in flow fields are observed. However, the situation may change drastically when anisotropic properties of the mushy zone, i.e. permeability and thermal conductivity, are accounted for, when thermo-solutal convection is included, different densities of the liquid and solid phase considered, other shape of the mould, different cooling conditions or solidification of other alloy studied. The latter conclusion may be drawn from results presented in Nandapurkar *et al.* (1991) where the case of upward moving directional solidification was considered and influence of the form of the momentum equation studied. Therefore, further comparison between different forms of the macroscopic equations, published in literature, should be continued in the future.

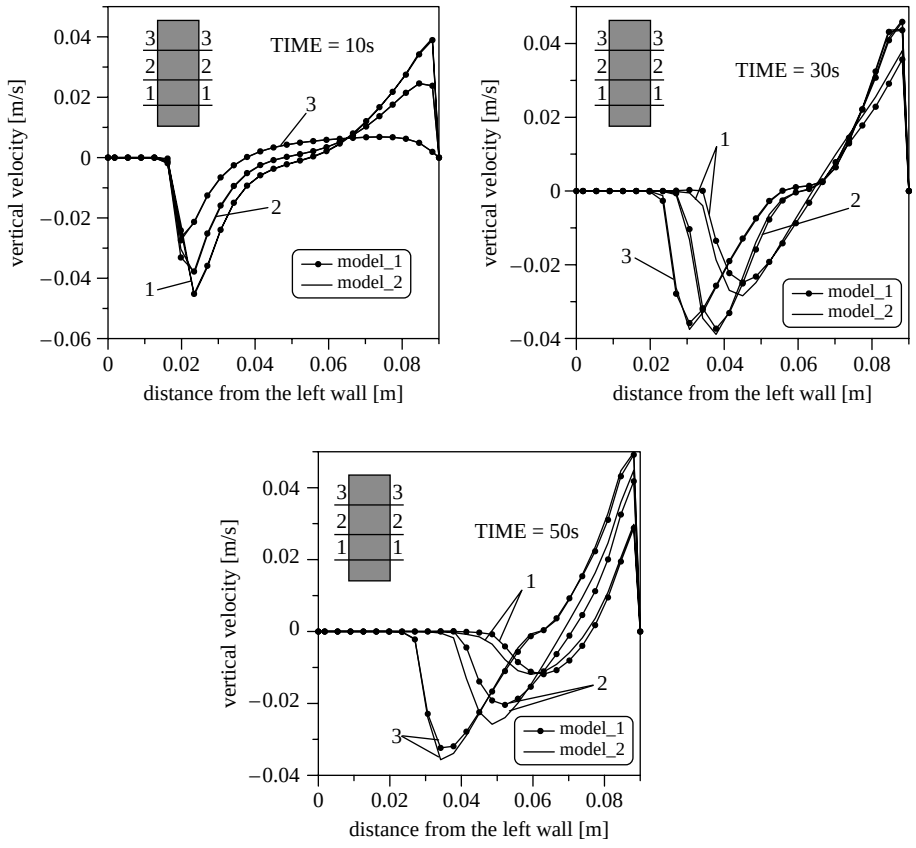

Figure 3.
Comparison of vertical component of the mixture velocity in three selected horizontal cross-sections for different models of the momentum equation in the mushy zone

References

Banaszek, J., Furmański, P. and Rebow, M. (2005), *Modelling of Transport Phenomena in Cooled and Solidifying Single Component and Binary Media*, Publishing House of the Warsaw University Technology, Warsaw.

Beckermann, C. and Viskanta, R. (1993), "Mathematical modelling of transport phenomena during alloy solidification", *Applied Mechanics Reviews*, Vol. 46, pp. 1-27.

Bennon, W.D. and Incropera, F.P. (1987), "A continuum model for momentum, heat and species transport in binary solid-liquid phase change systems – I. Model formulation", *Int. J. Heat & Mass Transfer*, Vol. 30, pp. 2161-70.

Bousquet-Melou, P., Goyeau, B., Quintard, M., Fichot, F. and Gobin, D. (2002), "Average momentum equation for interdendritic flow in a solidifying columnar mushy zone", *Int. J. Heat & Mass Transfer*, Vol. 45, pp. 3651-65.

Furmanski, P. (2004), *Microscopic-macroscopic Modeling of Transport Phenomena during Solidification in Heterogeneous Systems*, CISM Courses and Lectures No.449, Phase Change with Convection: Modelling and Validation, Springer Verlag, Wien, New York, NY, pp. 55-126.

Furmański, P. and Banaszek, J. (2006), "Modelling of the mushy zone permeability for solidification of binary alloys", *Materials Science Forum*, Vol. 508, pp. 411-8.

Ganesan, S. and Poirier, D.R. (1990), "Conservation of mass and momentum for the flow of interdendritic liquid during solidification", *Metallurgical Transactions B*, Vol. 21B, pp. 173-81.

Nandapurkar, P.J., Poirier, D.R. and Heinrich, J.C. (1991), "Momentum equation for dendritic solidification", *Numerical Heat Transfer A*, Vol. 19, pp. 297-311.

Patankar, S.V. (1980), *Numerical Heat Transfer and Fluid Flow*, Hemishere Publishing, Washington, DC.

Prescott, P.J., Incropera, F.P. and Bennon, W.D. (1991), "Modeling of dendritic solidification systems: reassessment of the continuum momentum equation", *Int. J. Heat & Mass Transfer*, Vol. 34, pp. 2351-9.

Sinha, S.K. and Sundarajan, T. (1992), "A variable property analysis of alloy solidification using the anisotropic porous medium approach", *Int. J. Heat & Mass Transfer*, Vol. 35, pp. 2865C-77C.

van Doormal, J.P. and Raithby, G.D. (1984), "Enhancements of the SIMPLE method for predicting incompressible fluid flows", *Numerical Heat Transfer*, Vol. 7, pp. 147-63.

Voller, V.R. and Swaminathan, C.R. (1992), "General enthalpy method for modelling solidification processes", *Metallurgical Transactions B*, Vol. 23B, pp. 651-64.

Corresponding author
Piotr Furmański can be contacted at: pfurm@itc.pw.edu.pl